PHYSICAL REVIEW D **82,** 023513 (2010)

Signature of cosmic string wakes in the CMB polarization

Rebecca J. Danos,* Robert H. Brandenberger,† and Gil Holder‡
Department of Physics, McGill University, Montréal, QC, H3A 2T8, Canada
(Received 3 April 2010; published 16 July 2010)

We calculate a signature of cosmic strings in the polarization of the cosmic microwave background. We find that ionization in the wakes behind moving strings gives rise to extra polarization in a set of rectangular patches in the sky whose length distribution is scale-invariant. The length of an individual patch is set by the comoving Hubble radius at the time the string is perturbing the cosmic microwave background. The polarization signal is largest for string wakes produced at the earliest post-recombination time, and for an alignment in which the photons cross the wake close to the time the wake is created. The maximal amplitude of the polarization relative to the temperature quadrupole is set by the overdensity of free electrons inside a wake which depends on the ionization fraction f inside the wake. For a cosmic string wake coming from an idealized string segment, the signal can be as high as 0.06 μK in degree scale polarization for a string at high redshift (near recombination) and a string tension μ given by $G\mu = 10^{-7}$.

DOI: 10.1103/PhysRevD.82.023513 PACS numbers: 98.80.Cq

I. INTRODUCTION

In recent years there has been renewed interest in the possibility that cosmic strings contribute to the power spectrum of curvature fluctuations which give rise to the large scale structure and cosmic microwave background (CMB) anisotropies which we see today. One of the reasons is that many inflationary models constructed in the context of supergravity models lead to the formation of gauge theory cosmic strings at the end of the inflationary phase [1]. Second, in a large class of brane inflation models the formation of cosmic superstrings [2] at the end of inflation is generic [3], and in some cases (see [4]) these strings are stable (see also [5] for reviews on fundamental cosmic strings). Cosmic superstrings are also a possible remnant of an early Hagedorn phase of string gas cosmology [6].

In models which admit stable strings or superstrings, a scaling solution of such strings inevitably [7] results as a consequence of cosmological dynamics (see e.g. [8] for reviews on cosmic strings and structure formation). In a scaling solution, the network of strings looks statistically the same at any time t if lengths are scaled to the Hubble radius at that time. The distribution of strings is dominated by a network of ''infinite'' strings[1] with mean curvature radius and separation being of the order of the Hubble radius. The scaling solution of infinite strings is maintained by the production of string loops due to the interaction of long strings. This leads to a distribution of string loops with a well-defined spectrum (see e.g. [9]) for all radii R smaller than a cutoff radius set by the Hubble length. Whereas the scaling distribution of the infinite strings is reasonably well known as a result of detailed numerical simulations of cosmic string evolution (see [10] for some references), there is still substantial uncertainty concerning the distribution of string loops. It is, however, quite clear that the long strings dominate the energy density of strings. The distinctive signals of strings which we will focus on are due to the long strings.

Cosmic strings give rise to distinctive signatures in both the CMB and in the large scale structure. These signatures are a consequence of the specific geometry of space produced by strings. As studied initially in [11], space perpendicular to a long straight string is locally flat but globally looks like a cone whose tip coincides with the location of the string (the smoothing out of the cone as a consequence of the internal structure of the cosmic string was worked out in [12]). The deficit angle is given by

$$\alpha = 8\pi G\mu, \tag{1}$$

where μ is the string tension and G is Newton's constant. Hence, a cosmic string moving with velocity v in the plane perpendicular to its tangent vector will lead to line discontinuities in the CMB temperature of photons passing on different sides of the string. The magnitude of the temperature jump is [13]

$$\frac{\delta T}{T} = 8\pi\gamma(v)vG\mu, \tag{2}$$

where γ is the relativistic gamma factor associated with the velocity v.

As a consequence of the deficit angle (1), a moving string will generate a cosmic string wake, a wedge-shaped region behind the string (from the point of view of its

*rjdanos@physics.mcgill.ca
†rhb@physics.mcgill.ca
‡holder@physics.mcgill.ca
[1]Any string with a mean curvature radius comparable or greater than the Hubble radius or which extends beyond the Hubble radius is called infinite or ''long.''

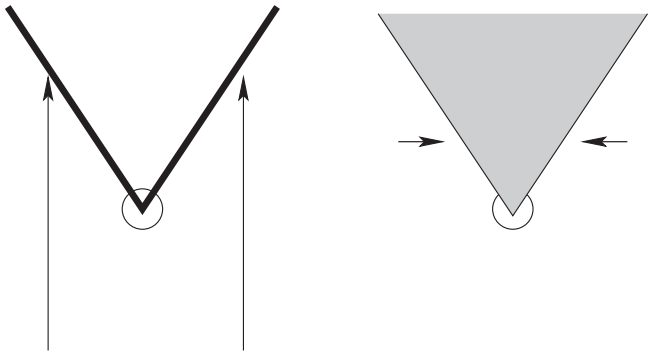

FIG. 1. Sketch of the mechanism by which a wake behind a moving string is generated. Consider a string perpendicular to the plane of the graph moving straight downward. From the point of view of the frame in which the string is at rest, matter is moving upwards, as indicated with the arrows in the left panel. From the point of view of an observer sitting behind the string (relative to the string motion) matter flowing past the string receives a velocity kick towards the plane determined by the direction of the string and the velocity vector (right panel). This velocity kick towards the plane leads to a wedge-shaped region behind the string with twice the background density (the shaded region in the right panel).

velocity), a region with twice the background density [14] (see Fig. 1). Causality (see e.g. [15]) limits the depth of the distortion of space due to a cosmic string. The details were worked out in [16] where it was shown that the deficit angle goes to zero quite rapidly a distance t from the string. Hence, the depth of the string wake is given by the same length. String wakes lead to distinctive signatures in the topology of the large-scale structure, signatures which were explored e.g. in [17].

Wakes formed at arbitrarily early times are nonlinear density perturbations. For wakes formed by strings present at times $t_i > t_{\rm rec}$, where $t_{\rm rec}$ is the time of recombination, the baryonic matter inside the wake undergoes shocks [18] (see e.g. [19] for a detailed study). The shocks, in turn, can ionize the gas—although as it turns out the residual ionization from decoupling is larger. Photons passing through these ionized regions on their way from the last scattering surface to the observer can thus be polarized—and it is this polarization signature which we aim to study here.

The tightest constraints on the contribution of scaling strings to structure formation (and thus the tightest upper bound on the tension μ of the strings) comes from the analysis of the angular power spectrum of CMB anisotropies. As discussed in [20–22], the angular power spectrum does not have the acoustic ringing which inflation-seeded perturbations generate. The reason is that the string network is continuously seeding the growing mode of the curvature fluctuation variable on super-Hubble scales. Hence, the fluctuations are ''incoherent'' and ''active'' as opposed to ''coherent'' and ''passive'' as in the case of inflation-generated fluctuations. The contribution of cosmic strings to the primordial power spectrum of cosmological perturbations is thus bounded from above, thus leading to an upper bound [23–27] on the string tension of between $G\mu < 3 \times 10^{-7}$ [23] and $G\mu < 7 \times 10^{-7}$ [26]. The analysis of [23] is based on a toy model for the scaling distribution of strings whereas [26] is based on numerical field theory simulations.

Past work on CMB temperature maps has shown that signatures of cosmic strings are easier to identify in position space than in Fourier space [13,28–30] and recent studies show that high angular resolution surveys such as the South Pole Telescope project [31] have the potential of improving the limits on the string tension by an order of magnitude [32–34] (although it must be mentioned that these analyses are based on a toy model distribution of cosmic strings which does not contain some features which emerge from numerical string network simulations [35] and which may render the sharp position space features harder to detect).

To date there has been little work on CMB polarization due to strings. Most of the existing work focuses on the angular power spectra of the polarization. Based on a formalism [22] (see also [36]) to include cosmic defects as source terms in the Boltzmann equations used in CMB codes, the power spectra of temperature and temperature polarization maps were worked out [37] in the case of models with global defects such as global cosmic strings. Since in cosmic defect models vector and tensor modes are as important as the scalar metric fluctuations [22,38], a significant B-mode polarization is induced. In fact, in the case of global strings with a tension close to the upper bound mentioned above, whereas the amplitude of the temperature and E-mode polarization power spectra are so small as to make the string signal invisible compared to the signal from the scale-invariant spectrum of adiabatic fluctuations (e.g. produced in inflation), the contribution of strings dominates the amplitude of the B-mode polarization power spectrum. In the case of local strings, these conclusions were confirmed in the more recent analyses of [23,26,27,39,40]. The maximal amplitude of the B-mode polarization power spectrum for strings with $G\mu = 3 \times 10^{-7}$ was shown to be taken on at angular harmonic values of $l \sim 500$ and to be of the order 0.3 μK^2 [40]. However, the analyses of [23,26,27,39,40] do not take into account the effects of the gravitational accretion onto cosmic string wakes. In related work, the conversion of E-mode to B-mode polarization via the gravitational lensing induced by cosmic strings was studied in [41].[2]

Similarly to what was found in the analysis of CMB temperature maps from cosmic strings, we expect that a position-space analysis will be more powerful at revealing

[2]While this paper was being finalized for submission, a preprint appeared [42] computing the local B-mode polarization power spectrum from cosmic strings.

the key non-Gaussian signatures of strings in CMB polarization. Hence, in this work we derive the position space signature of a cosmic string wake in CMB polarization maps.

In the following section we briefly review cosmic string wakes. In Sec. III we then analyze the polarization signature of wakes, and we conclude with some discussion.

II. COSMIC STRING WAKES

Since the strings are relativistic, they generally move with a velocity of the order of the speed of light. There will be frequent intersections of strings. The long strings will chop off loops, and this leads to the conclusion that the string distribution will be statistically independent on time scales larger than the Hubble radius.[3]

In this work, we place one string of length $c_1 t_i$[4] at a specified time t_i and assume it is moving in transverse direction with a velocity v_s. This string segment will generate a wake, and it is the signal of one of these wakes in the CMB polarization which we will study in the following.

A string segment laid down at time t_i. will generate a wake whose dimensions at that time are the following:

$$c_1 t_i \times t_i v_s \gamma_s \times 4\pi G \mu t_i v_s \gamma_s. \tag{3}$$

In the above, the first dimension is the length in direction of the string, the second is the depth which depends on v_s (γ_s is the associated relativistic γ factor), and the third is the average thickness. The geometry of a cosmic string wake is illustrated in Fig. 2.

Once the wake is formed, its planar dimensions will expand as the universe grows in size, and the thickness (defined as the region of nonlinear density) will grow by gravitational accretion. The accretion of matter onto a cosmic string wake was studied in [44,45] in the case of the dark matter being cold, and in [45,46] in the case of the dark matter being hot.[5] We are interested in the case of cold dark matter.

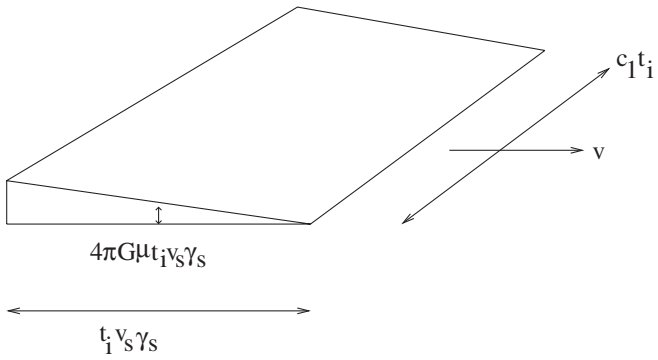

FIG. 2. Sketch of the geometry of a cosmic string wake. The wake is the wedge-shaped region shown. The string is moving in horizontal direction towards the right, and is located along the line where the wake has vanishing thickness. The horizontal dimension of the wake is determined by the string velocity and the Hubble time when the wake is created (time t_i). The size of the wake in direction of the string is set by the curvature radius of the cosmic string network and is in our toy model taken to be the Hubble scale. The thickness of the wake perpendicular to the plane spanned by the tangent vector of the string and the string velocity vector changes as we move away from the tip of the string. The average wake thickness is indicated by the short vertical line with arrow signs in both directions.

We consider mass planes at a fixed initial comoving distance q above the center of the wake. The corresponding physical height is

$$h(q, t) = a(t)[q - \psi(q, t)], \tag{4}$$

where $\psi(q, t)$ is the comoving displacement induced by the gravitational accretion onto the wake. For cold dark matter, the initial conditions for $\psi(q)$ are $\psi(q, t_i) = \psi(\dot{q}, t_i) = 0$. The goal of the analysis is to find the thickness of the wake at all times $t > t_i$. The thickness is defined as the physical height h above the center of the wake of the matter shell which is beginning to fall towards the wake, i.e. for which $h(\dot{q}, t) = 0$. In the Zel'dovich approximation, we first consider the equation of motion for h obtained by treating the source (the initial surface density σ of the wake) in the Newtonian limit, i.e.

$$\ddot{h} = -\frac{\partial \Phi}{\partial h}, \tag{5}$$

where Φ is the Newtonian gravitational potential given by the Poisson equation

[3]Hence, to model the effects of strings we will make use of a toy model introduced in [43] and used in most analytical work on cosmic strings and structure formation since then: we divide the time interval between recombination and the current time t_0 into Hubble expansion time steps. In each time step, we will approximate the infinite strings by a collection of finite straight string segments whose length is given by the curvature radius of the string network. On a Hubble time scale, the infinite strings will self-intersect. Hence, we take the distribution of string segments to be statistically independent on a Hubble time scale. Hence, in each time step there is a distribution of straight string segments moving in randomly chosen directions with velocities chosen at random between 0 and 1 (in units of the speed of light). The centers and directions of these string segments are random, and the string density corresponds to N strings per Hubble volume, where N is an integer which is of the order 1 according to the scaling of the string network. The distribution of string segments is uncorrelated at different Hubble times.

[4]The constant c_1 is of the order 1 and depends on the correlation length of the string network as a function of the Hubble radius and must be determined from numerical simulations of cosmic string evolution.

[5]If the strings have lots of small-scale structure then they will have an effective tension which is less than the effective energy density [47]. This will lead to a local gravitational attraction of matter towards the string, a smaller transverse velocity, and hence to string filaments instead of wakes. The gravitational accretion onto string filaments was studied in [48].

$$\frac{\partial^2\Phi}{\partial^2 h} = 4\pi G[\rho + \sigma\delta(h)] \tag{6}$$

[$\rho(t)$ being the background energy density], and then by linearizing the resulting equation in ψ. The mean surface density is

$$\sigma(t) = 4\pi G\mu t_i v_s \gamma_s \left(\frac{t}{t_i}\right)^{2/3} \rho(t). \tag{7}$$

The result of the computation of the value of the comoving displacement q_{nl} which is ''turning around'' at the time t for a wake laid down at time t_i is [45]

$$q_{nl}(t, t_i) = \psi_0 \left(\frac{t}{t_i}\right)^{2/3} \tag{8}$$

with

$$\psi_0(t_i) = \frac{24\pi}{5} G\mu v_s \gamma_s (z(t_i) + 1)^{-1/2} t_0. \tag{9}$$

This corresponds to a physical height of

$$h(t, t_i) = a(t)[q_{nl}(t, t_i) - \psi(q_{nl}, t)] \simeq a(t) q_{nl}(t, t_i) = \psi_0 \frac{z_i + 1}{(z + 1)^2}, \tag{10}$$

where z_i and z are the redshifts corresponding to the times t_i and t, respectively. These formulas agree with what is expected from linear cosmological perturbation theory: the fractional density perturbation should increase linearly in the scale factor which means that the comoving width of the wake must grow linearly with $a(t)$.[6] It should be emphasized that the above result (10) assumes a wake created by an idealized straight string segment.

Let us return to the geometry of the string segment. The tangent vector to the string and the direction of motion of the string determine a surface in space (the ''string plane''). If neither the string tangent vector nor the velocity vector have a radial component (radial with respect to the comoving point of our observer), then the photons will cross each point of the string wake at the same time, and the wake will correspond to a rectangle in the sky whose planar dimensions are

$$c_1 t_1 \times t_i v_s \gamma_s. \tag{11}$$

However, if the normal vector of the string plane is not radial, then one of the planar dimensions will be reduced by a trigonometric factor $\cos(\theta)$ depending on the angle θ between the normal vector and the radial vector. In addition, photons which we detect today did not pass the wake at the same time. This will lead to a gradient of the polarization signal across the projection of the wake onto the CMB sky. To simplify the analysis, in the following we will assume that θ is small.

[6]This formula agrees within a factor of 2 with the numerical studies of [19].

In the following section we will need the expression for the number density $n_e(t, t_i)$ of free electrons at time t in a wake which was laid down at the time t_i. The initial number density is

$$n_e(t_i, t_i) \simeq f\rho_B(t_i) m_p^{-1}, \tag{12}$$

where f is the ionization fraction, ρ_B is the energy density in baryons, and m_p is the proton mass. Taking into account that for $t > t_i$ the number density redshifts as the inverse volume we get

$$n_e(t, t_i) \simeq f\rho_B(t_i) m_p^{-1} \left(\frac{z(t) + 1}{z(t_i) + 1}\right)^3. \tag{13}$$

III. ANALYSIS

If unpolarized cosmic microwave background radiation with a quadrupolar anisotropy scatters off free electrons, then the scattered radiation is polarized (see e.g. [49] for reviews of the theory of CMB polarization). The magnitude of the polarization depends on the Thomson cross section σ_T and on the integral of the number density of electrons along the null geodesic of radiation. Our starting formula is

$$P(\mathbf{n}) \simeq \frac{1}{10}\left(\frac{3}{4\pi}\right)^{1/2} \tau_T Q, \tag{14}$$

where $P(\mathbf{n})$ is the magnitude of polarization of radiation from the direction $\mathbf{n}$, Q is the temperature quadrupole, and

$$\tau_T = \sigma_T \int n_e(\chi) d\chi, \tag{15}$$

where the integral is along the null geodesic in terms of conformal time.

Let us now estimate the contribution to the polarization amplitude from CMB radiaton passing through a single wake at time t, assuming that the wake was laid down at the time t_i and has thus had time to grow from time t_i to the time t when the photons are crossing it. We assume that the photons cross in perpendicular direction. Since the wake is thin, we can estimate the integral in Eq. (15) by

$$\tau_T \sim 2\sigma_T n_e(t, t_i)(z(t) + 1) h(t, t_i), \tag{16}$$

where the factor 2 is due to the fact that the width of the wake is twice the height, and the redshift factor comes from the Jacobean transformation between χ and position. Inserting Eq. (16) into the expression (14) for the polarization amplitude and using the value for the height and the number density of electrons obtained in the previous section we find

$$\frac{P}{Q} \simeq \frac{1}{5}\left(\frac{3}{4\pi}\right)^{1/2} \sigma_T f\rho_B(t_i) m_p^{-1} \frac{(z(t) + 1)^2}{(z(t_i) + 1)^2} \psi_0(t_i). \tag{17}$$

Inserting the formula for $\psi_0(t_i)$ from Eq. (9), expressing the baryon density at t_i in terms of the current baryon

density, and the latter in terms of the baryon fraction Ω_B and the total energy density ρ_c at the current time t_0, we obtain

$$\frac{P}{Q} \simeq \frac{24\pi}{25}\left(\frac{3}{4\pi}\right)^{1/2}\sigma_T f G\mu v_s\gamma_s \times \Omega_B\rho_c(t_0)m_p^{-1}t_0(z(t)+1)^2(z(t_i)+1)^{1/2}. \quad (18)$$

From Eq. (18) we see that the polarization signal is larger for wakes laid down early, i.e. close to the time of recombination. For fixed t_i, the signal is largest for configurations where the photons we observe today cross the wake at the earliest possible time, i.e. for the largest $z(t)$ (obviously, t is constrained to be larger than t_i, otherwise our formula for the height is not applicable). To get an order of magnitude estimate of the magnitude of the polarization signal, we take $z(t_i) \sim z(t) \sim 10^3$. Inserting the value of the Thomson cross section, the proton mass and the current time we get

$$\frac{P}{Q} \sim f G\mu v_s\gamma_s\Omega_B\left(\frac{z(t)+1}{10^3}\right)^2\left(\frac{z(t_i)+1}{10^3}\right)^3 \times 10^7. \quad (19)$$

The ionization fraction of baryonic matter drops off after recombination, but it does not go to zero. As already discussed in [50,51] there is remnant residual ionization of the matter. As computed in [51] (see also [52]), the residual ionization fraction f tends to a limiting value of between 10^{-5} and 10^{-4} at late times after recombination.

Shocks inside the wake will lead to extra ionization. However, the resulting contribution to the ionization fraction is negligible for the range of string tensions we are interested in. To see this, we follow the analysis of [18]. A particle streaming towards a cosmic string wake has velocity

$$v_i = 4\pi G\mu v_s\gamma_s \quad (20)$$

and kinetic energy $\frac{1}{2}mv_i^2$. The particles will undergo shocks and thermalize. Equating the initial kinetic energy density with the final thermal energy density (assuming that the particles are distributed according to an approximate ideal gas law) yields a temperature inside the wakes of

$$T \simeq 7\times 10^3\left(\frac{G\mu}{2\times 10^{-6}}\right)^2(v_s\gamma_s)^2 \text{ K}. \quad (21)$$

We then compute the Boltzmann factor to determine the ratio of ionized Hydrogen to ground state Hydrogen which is the ionization fraction. For string tensions of order 10^{-6} this results in ionization fractions of the order 10^{-9} which is considerably less than the residual ionization. For more realistic string tensions compatible with current bounds, 10^{-7}, the ionization fraction due to shocks is negligible compared to the residual ionization fraction. At the temperatures considered for a string tension of 10^{-7} at lower redshifts there would be star formation and hence an ionization fraction due to that effect since the wake would contain molecular hydrogen and satisfy the appropriate conditions. However, this is not an issue at redshifts under consideration.

Note that even though the extra ionization inside the wake is negligible compared to the overall ionization level, the wake is a locus of extra energy density. Thus, even if the ionization fraction is homogeneous in space, the inhomogeneous distribution of matter will lead to a specific polarization signature.

The position space signal of the polarization produced by a wake will be very specific: for a wake whose normal vector is in radial direction, it will be a rectangle in the sky with angular dimensions corresponding to the comoving size

$$c_1 t_i(z(t_i)+1) \times v_s\gamma_s t_i(z(t_i)+1) \quad (22)$$

[see Eq. (3)]. If the angle of the normal of the string plane to the radial normal vector is $\theta \neq 0$, then one of the planar dimensions is reduced by a factor of $\cos(\theta)$. However, the light travel time through the wake is increased by a factor of $[\cos(\theta)]^{-1}$. Thus, the wake becomes a bit smaller but the signal strength increases. The average amplitude of the polarization is given by Eq. (18)—a value obtained using the average thickness of the wake. However, since the thickness of the wake increases linearly in direction of the string motion, the amplitude of the polarization signal will also increase linearly in this direction. A second source for the linear increase in the amplitude is the fact that $z(t_i)$ is increasing as we go away from the tip of the cone (by an amount corresponding to one Hubble expansion time when comparing the tip of the cone to the end). The direction of the polarization vector depends on the relative orientation between the string and the CMB quadrupole. In Fig. 3 we give a sketch of the signal. The amplitude of the polarization is proportional to the length of the arrow, the direction of the polarization is given by the direction of the arrow. Since the direction of the variation of the polarization strength is determined by the string and is therefore uncorrelated with the direction of the CMB quadrupole, on the average the E-mode and B-mode strengths of the polarization signal will be the same.

Let us now discuss the magnitude of our effect. We will consider the value $G\mu = 3\times 10^{-7}$ which is the current upper bound on the string tension [23] (using the assumptions about the cosmic string scaling solution made in these papers). Wakes produced close to the time of recombination inherit the ionization fraction of the universe at that time. Taking a value of $f = 10^{-3}$ (which is smaller than the ionization fraction until redshift $z \simeq 600$ [52]), we obtain a polarization amplitude of $P \sim 10^{-2}$ μK which is larger than the background in the B-mode polarization arising from weak lensing of the primordial perturbations [53,54] for l-values of about 100.

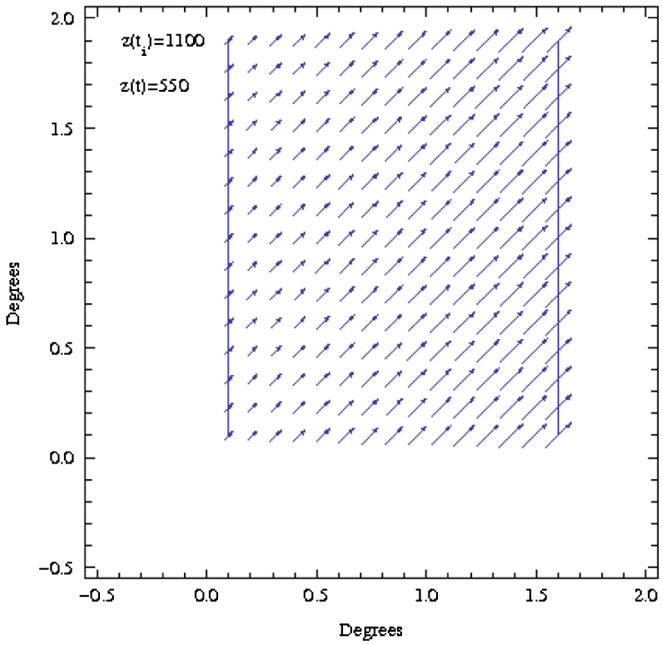

FIG. 3 (color online). The polarization signal of a single wake which is taken to be perpendicular to the line of sight between us and the center of the string segment. The tip of the wake (position of the string at the time the wake is laid down) is the vertical edge of the rectangle, and the string velocity vector is pointing horizontally to the left The length and direction of the arrows indicate the magnitude and orientation of the polarization vector. We have assumed that the variation of the quadrupole vector across the plane of the wake is negligible. Note that the angle between the velocity vector of the string and the CMB quadrupole is random. We have assumed that the quadrupole vector is at an angle relative to the plane of the wake. This determines the direction of the polarization vector we have drawn. The orientation we have chosen in this figure corresponds to an almost pure B-mode.

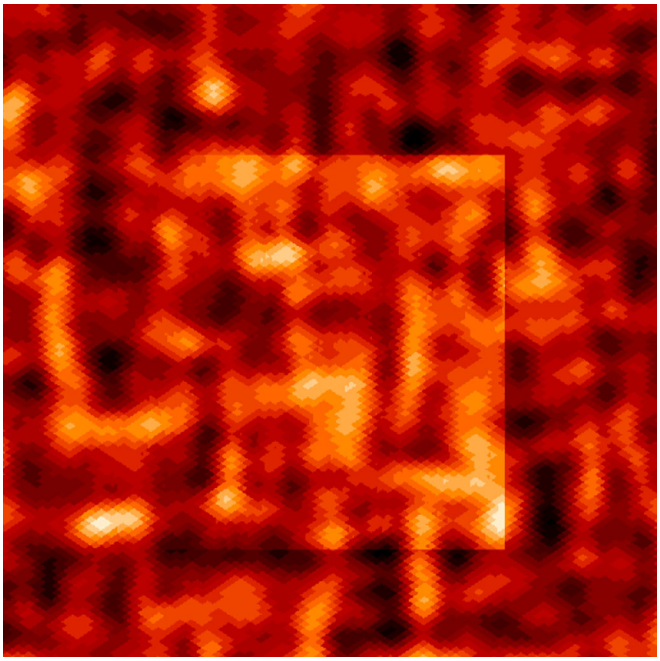

FIG. 4 (color online). The Q-mode polarization signal of a single wake which is taken to be perpendicular to the line of sight between us and the center of the string segment, superimposed on the Gaussian noise signal which is expected to dominate the total power spectrum. The string signal is multiplied by a factor of 100 to render it visible by eye. The tip of the wake (position of the string at the time the wake is laid down) is the vertical bright edge of the right side, and the string velocity vector is pointing horizontally to the left. At the final string position the wake thickness vanishes and there is no polarization discontinuity line. We have assumed that the variation of the quadrupole vector across the plane of the wake is negligible and that the quadrupole vector is at an angle relative to the plane of the wake such that the Q-mode picks up half of the polarization power.

It is instructive to compare our polarization signal from a cosmic string wake with the expected noise due to the Gaussian fluctuations. In Fig. 4 we have superimposed the map of the Q-mode polarization from a cosmic string wake laid down during the first Hubble time after recombination with a corresponding Q-mode map due to Gaussian noise of the concordance ΛCDM model. The string parameters are the same as mentioned in the previous paragraph. We chose the orientation of the string relative to the CMB quadrupole such that the power in the Q-mode is half the total power. As the value of the CMB quadrupole we used 30 μK. To render the string signal visible in the Q-mode map (in which the noise is much larger than in a B-mode map) we multiplied the string signal by 100. In this case the string signal is clearly visible be eye. The brightest edge (the vertical edge on the right side) corresponds to the position of the string when it begins to generate the wake, not at the position at the end of the time interval being considered (the vertical edge on the left). Note the difference compared to the Kaiser-Stebbins effect in the CMB temperature maps: in this case the brightest edge corresponds to the location of the string when the photons are passing by it.

Without boosting the string signal by a large factor, it would not be visible by eye. However, the distinctive lines in the map can be searched for by edge detection algorithms such as the Canny algorithm which was used to study the string signal in CMB temperature maps. In the studies of [34] it was found that the cosmic string lines in temperature maps can be picked out if the string signal accounts for less than 0.2% of the power. Thus, it should be able to easily pick out the string signal in the Q-mode polarization maps. In B-mode polarization maps the string signal would be much easier to detect.

IV. CONCLUSIONS AND DISCUSSION

In this Letter we have discussed a position space signal of a cosmic string wake in CMB polarization maps. In the same way that the line discontinuities in the CMB temperature maps predicted by the Kaiser-Stebbins (KS) effect

yield a promising way to constrain/detect cosmic strings in the CMB (see e.g. [28–30,32–34]), we believe that the signal discussed in this paper will play a similar role once CMB polarization maps become available.

We have shown that a single wake will produce a rectangular patch in the sky of dimensions given by Eq. (22), average magnitude given by Eq. (18) and amplitude increasing linearly in one direction across the patch. For a value of the string tension $G\mu = 3 \times 10^{-7}$ (the current upper limit), the amplitude of the signal is within the range of planned polarization experiments for wakes produced sufficiently close to the surface of recombination. These wakes are also the most numerous ones. The brightest edge in the polarization map corresponds to the beginning location of the string, not the final location. Since the KS discontinuity in the CMB temperature map will occur along the line corresponding to the final position, the polarization signal discussed here provides a cross check on a possible string interpretation of a KS signal.

A scaling distribution of strings will yield a distribution of patches in the sky, the most numerous ones and the ones with the largest polarization amplitude being set by wakes laid down at times close to the time of recombination which are crossed by the CMB photons at similarly early times.

ACKNOWLEDGMENTS

This work is supported in part by a NSERC Discovery Grants and by funds from the CRC Program to R. B. and G. H. and by CIfAR (G. H.). We thank Andrew Frey, Oscar Hernandez and J. Magueijo for useful discussions.

[1] R. Jeannerot, Phys. Rev. D **53**, 5426 (1996); R. Jeannerot, J. Rocher, and M. Sakellariadou, Phys. Rev. D **68**, 103514 (2003).
[2] E. Witten, Phys. Lett. **153B**, 243 (1985).
[3] S. Sarangi and S. H. H. Tye, Phys. Lett. B **536**, 185 (2002).
[4] E. J. Copeland, R. C. Myers, and J. Polchinski, J. High Energy Phys. 06 (2004) 013.
[5] A. C. Davis and T. W. B. Kibble, Contemp. Phys. **46**, 313 (2005); M. Sakellariadou, Phil. Trans. R. Soc. A **366**, 2881 (2008).
[6] R. H. Brandenberger and C. Vafa, Nucl. Phys. **B316**, 391 (1989); A. Nayeri, R. H. Brandenberger, and C. Vafa, Phys. Rev. Lett. **97**, 021302 (2006); R. H. Brandenberger, A. Nayeri, S. P. Patil, and C. Vafa, Int. J. Mod. Phys. A **22**, 3621 (2007); R. H. Brandenberger, arXiv:0808.0746.
[7] T. W. B. Kibble, Acta Phys. Pol. B **13**, 723 (1982); Phys. Rep. **67**, 183 (1980).
[8] A. Vilenkin and E. P. S. Shellard, *Cosmic Strings and Other Topological Defects* (Cambridge University Press, Cambridge, England, 1994); M. B. Hindmarsh and T. W. Kibble, Rep. Prog. Phys. **58**, 477 (1995); R. H. Brandenberger, Int. J. Mod. Phys. A **9**, 2117 (1994).
[9] N. Turok and R. H. Brandenberger, Phys. Rev. D **33**, 2175 (1986); H. Sato, Prog. Theor. Phys. **75**, 1342 (1986); A. Stebbins, Astrophys. J. Lett. **303**, L21 (1986).
[10] A. Albrecht and N. Turok, Phys. Rev. Lett. **54**, 1868 (1985); D. P. Bennett and F. R. Bouchet, Phys. Rev. Lett. **60**, 257 (1988); B. Allen and E. P. S. Shellard, Phys. Rev. Lett. **64**, 119 (1990); C. Ringeval, M. Sakellariadou, and F. Bouchet, J. Cosmol. Astropart. Phys. 02 (2007) 023; V. Vanchurin, K. D. Olum, and A. Vilenkin, Phys. Rev. D **74**, 063527 (2006).
[11] A. Vilenkin, Phys. Rev. D **23**, 852 (1981).
[12] R. Gregory, Phys. Rev. Lett. **59**, 740 (1987).
[13] N. Kaiser and A. Stebbins, Nature (London) **310**, 391 (1984).
[14] J. Silk and A. Vilenkin, Phys. Rev. Lett. **53**, 1700 (1984).
[15] J. H. Traschen, Phys. Rev. D **29**, 1563 (1984); **31**, 283 (1985).
[16] J. C. R. Magueijo, Phys. Rev. D **46**, 1368 (1992).
[17] R. H. Brandenberger, D. M. Kaplan, and S. A. Ramsey, arXiv:astro-ph/9310004; D. Mitsouras, R. H. Brandenberger, and P. Hickson, arXiv:astro-ph/9806360.
[18] M. Rees, Mon. Not. R. Astron. Soc. **222**, 27 (1986).
[19] A. Sornborger, R. H. Brandenberger, B. Fryxell, and K. Olson, Astrophys. J. **482**, 22 (1997).
[20] L. Perivolaropoulos, Astrophys. J. **451**, 429 (1995).
[21] J. Magueijo, A. Albrecht, D. Coulson, and P. Ferreira, Phys. Rev. Lett. **76**, 2617 (1996).
[22] U. L. Pen, U. Seljak, and N. Turok, Phys. Rev. Lett. **79**, 1611 (1997).
[23] L. Pogosian, S. H. H. Tye, I. Wasserman, and M. Wyman, Phys. Rev. D **68**, 023506 (2003); **73**, 089904(E) (2006); M. Wyman, L. Pogosian, and I. Wasserman, Phys. Rev. D **72**, 023513 (2005); **73**, 089905(E) (2006).
[24] A. A. Fraisse, J. Cosmol. Astropart. Phys. 03 (2007) 008.
[25] U. Seljak, A. Slosar, and P. McDonald, J. Cosmol. Astropart. Phys. 10 (2006) 014.
[26] N. Bevis, M. Hindmarsh, M. Kunz, and J. Urrestilla, Phys. Rev. D **75**, 065015 (2007); Phys. Rev. Lett. **100**, 021301 (2008).
[27] R. A. Battye, B. Garbrecht, and A. Moss, J. Cosmol. Astropart. Phys. 09 (2006) 007; R. A. Battye, B. Garbrecht, A. Moss, and H. Stoica, J. Cosmol. Astropart. Phys. 01 (2008) 020.
[28] R. Moessner, L. Perivolaropoulos, and R. H. Brandenberger, Astrophys. J. **425**, 365 (1994).
[29] A. S. Lo and E. L. Wright, arXiv:astro-ph/0503120.
[30] E. Jeong and G. F. Smoot, Astrophys. J. **624**, 21 (2005); arXiv:astro-ph/0612706.
[31] J. E. Ruhl *et al.* (The SPT Collaboration), Proc. SPIE Int. Soc. Opt. Eng. **5498**, 11 (2004).
[32] S. Amsel, J. Berger, and R. H. Brandenberger, J. Cosmol. Astropart. Phys. 04 (2008) 015.

[33] A. Stewart and R. Brandenberger, J. Cosmol. Astropart. Phys. 02 (2009) 009.
[34] R. J. Danos and R. H. Brandenberger, Int. J. Mod. Phys. D **19**, 183 (2010); J. Cosmol. Astropart. Phys. 02 (2010) 033.
[35] A. A. Fraisse, C. Ringeval, D. N. Spergel, and F. R. Bouchet, Phys. Rev. D **78**, 043535 (2008).
[36] A. J. Albrecht, R. A. Battye, and J. Robinson, Phys. Rev. D **59**, 023508 (1998).
[37] U. Seljak, U. L. Pen, and N. Turok, Phys. Rev. Lett. **79**, 1615 (1997).
[38] R. Durrer, M. Kunz, and A. Melchiorri, Phys. Rev. D **59**, 123005 (1999).
[39] U. Seljak and A. Slosar, Phys. Rev. D **74**, 063523 (2006).
[40] L. Pogosian, I. Wasserman, and M. Wyman, arXiv:astro-ph/0604141; L. Pogosian and M. Wyman, Phys. Rev. D **77**, 083509 (2008).
[41] K. Benabed and F. Bernardeau, Phys. Rev. D **61**, 123510 (2000).
[42] J. Garcia-Bellido, R. Durrer, E. Fenu, D. G. Figueroa, and M. Kunz, arXiv:1003.0299.
[43] L. Perivolaropoulos, Phys. Lett. B **298**, 305 (1993); Phys. Rev. D **48**, 1530 (1993).
[44] A. Stebbins, S. Veeraraghavan, R. H. Brandenberger, J. Silk, and N. Turok, Astrophys. J. **322**, 1 (1987).
[45] R. H. Brandenberger, L. Perivolaropoulos, and A. Stebbins, Int. J. Mod. Phys. A **5**, 1633 (1990).
[46] L. Perivolaropoulos, R. H. Brandenberger, and A. Stebbins, Phys. Rev. D **41**, 1764 (1990).
[47] B. Carter, Phys. Rev. D **41**, 3869 (1990); A. Vilenkin, Phys. Rev. D **41**, 3038 (1990).
[48] A. N. Aguirre and R. H. Brandenberger, Int. J. Mod. Phys. D **4**, 711 (1995).
[49] W. Hu, Astrophys. J. **529**, 12 (2000); O. Dore, G. Holder, M. Alvarez, I. T. Iliev, G. Mellema, U. L. Pen, and P. R. Shapiro, Phys. Rev. D **76**, 043002 (2007).
[50] I. D. Novikov and Y. B. Zeldovic, Annu. Rev. Astron. Astrophys. **5**, 627 (1967).
[51] P. J. E. Peebles, Astrophys. J. **153**, 1 (1968).
[52] M. Kaplinghat, M. Chu, Z. Haiman, G. Holder, L. Knox, and C. Skordis, Astrophys. J. **583**, 24 (2003).
[53] C. M. Hirata and U. Seljak, Phys. Rev. D **68**, 083002 (2003).
[54] G. P. Holder, K. M. Nollett, and A. van Engelen, Astrophys. J. **716**, 907 (2010).